AIP Advances

High pressure synthesis of amorphous TiO_2 nanotubes

Cite as: AIP Advances **5**, 097128 (2015); https://doi.org/10.1063/1.4930916
Submitted: 22 April 2015 . Accepted: 27 August 2015 . Published Online: 09 September 2015

Quanjun Li, Ran Liu, Tianyi Wang, Ke Xu, Qing Dong, Bo Liu, Jing Liu, and Bingbing Liu

View Online Export Citation CrossMark

ARTICLES YOU MAY BE INTERESTED IN

Pressure-induced amorphization in orthorhombic Ta_2O_5: An intrinsic character of crystal
Journal of Applied Physics **115**, 193512 (2014); https://doi.org/10.1063/1.4879245

Effect of annealing temperature of titanium dioxide thin films on structural and electrical properties
AIP Conference Proceedings **1788**, 030030 (2017); https://doi.org/10.1063/1.4968283

Anomalous compression behavior of ~12 nm nanocrystalline TiO_2
Journal of Applied Physics **121**, 215109 (2017); https://doi.org/10.1063/1.4984918

AVS Quantum Science
Co-Published by AIP Publishing AVS
RECEIVE THE LATEST UPDATES

© 2015 Author(s).

High pressure synthesis of amorphous TiO_2 nanotubes

Quanjun Li,[1] Ran Liu,[1] Tianyi Wang,[1] Ke Xu,[1] Qing Dong,[1] Bo Liu,[1] Jing Liu,[2] and Bingbing Liu[1,a]
[1]*State Key Laboratory of Superhard Materials, Jilin University, Changchun 130012, China*
[2]*Institute of High Energy Physics, Chinese Academy of Sciences, Beijing 100049, China*

(Received 22 April 2015; accepted 27 August 2015; published online 9 September 2015)

Amorphous TiO_2 nanotubes with diameters of 8-10 nm and length of several nanometers were synthesized by high pressure treatment of anatase TiO_2 nanotubes. The structural phase transitions of anatase TiO_2 nanotubes were investigated by using in-situ high-pressure synchrotron X-ray diffraction (XRD) method. The starting anatase structure is stable up to ~20GPa, and transforms into a high-density amorphous (HDA) form at higher pressure. Pressure-modified high- to low-density transition was observed in the amorphous form upon decompression. The pressure-induced amorphization and polyamorphism are in good agreement with the previous results in ultrafine TiO_2 nanoparticles and nanoribbons. The relationship between the LDA form and α-PbO_2 phase was revealed by high-resolution transmission electron microscopy (HRTEM) study. In addition, the bulk modulus (B_0 = 158 GPa) of the anatase TiO_2 nanotubes is smaller than those of the corresponding bulks and nanoparticles (180-240 GPa). We suggest that the unique open-ended nanotube morphology and nanosize play important roles in the high pressure phase transition of TiO_2 nanotubes. © *2015 Author(s). All article content, except where otherwise noted, is licensed under a Creative Commons Attribution 3.0 Unported License.* [http://dx.doi.org/10.1063/1.4930916]

I. INTRODUCTION

Nanotubes have attracted considerable attention because of their interesting electronic, mechanical, and structural properties.[1–3] Among the different classes of nanotubes, TiO_2 nanotube is one of the most typical model which exhibit promising applications in photocatalysis, gas sensors, lithium-ions battery, and so on.[3–6] Highly ordered transparent TiO_2 nanotube arrays showed superior electron lifetimes and provided excellent pathways for electron percolation in dye-sensitized solar cells.[7] TiO_2 nanotubes with large surface areas exhibited relatively large reversible capacity and good reversibility in electrochemical lithium storage.[4] TiO_2 nanotubes and their hybrids with other materials also showed excellent photocatalytic properties due to their high absorption ability of nanotubular morphology and nanosize.[8–10] In addition, open-ended TiO_2 nanotubes provide internal cavities that are capable of accommodating biomolecules of suitable size and liquids. Unique physical phenomena and physicochemical reactions would occur in the defined nanosize channels. Therefore, the structural study of the nanotubes is very important to realize their properties and is of great benefit to their proper applications. There remains a need for a further structural investigation of TiO_2 nanotubes under various conditions.

Synthesis of nanostructured materials is a hot topic over the past decades. Previous studies have proved that materials' properties can be modified largely by their nanostructures. Various nanomaterials with special morphology were synthesized by different physical and chemical methods. Recently, high pressure has proved to be an efficient method for preparing nanomaterials with novel high pressure phase.[11,15] For instance, ultrahard nanotwinned cubic boron nitride and diamond have been

[a]Author to whom correspondence should be addressed. Electronic mail: liubb@jlu.edu.cn.

 © Author(s) 2015

synthesized by high temperature and high pressure treatment of onion-like BN precursor nanoparticles and onion carbon nanoparticles.[11,12] TiO_2 nanosheets, nanowires and nanoporous structure with high pressure phase of α-PbO_2 were obtained after the high pressure treatment.[14,15] Moreover, amorphous nanoribbons and nanorods have been prepared in TiO_2 and Gd_2O_3, respectively.[13,16] Pressure-induced amorphization in PbTe,[17] Y_2O_3[18] and TiO_2[19–21] nanoparticles provides a potential way to synthesize novel amorphous nanomaterials from the corresponding nanocrystals. As is well known, amorphous materials have unique isotropy because of the absence of long-range ordered crystal structure, which are unsubstituted by crystals in many fields. Amorphous nanomaterials also exhibited interesting physicochemical properties and attracted more and more attention. However, synthesis of amorphous nanomaterials with special morphology is still a challenge because the most morphology of nanocrystals is related to their crystal structural characters which do not exist in amorphous materials. High pressure provides a potential route for preparing nanostructured amorphous materials from the corresponding crystal nanomaterials by using their pressure-induced amorphization. TiO_2 nanomaterials show unique size- and morphology-dependent phase transition behaviors under high pressure, especially for their pressure-induced amorphization in ultrafine nanoparticles[19–21] and nanostructures.[13] This motivates us to study the phase transition behaviors and synthesize amorphous TiO_2 nanotubes under high pressure.

In this work, we synthesized the amorphous TiO_2 nanotubes by high pressure treatment of anatase TiO_2 nanotubes. The high pressure behaviors of the TiO_2 nanotubes were studied by in-situ high-pressure synchrotron XRD and HRTEM techniques. PIA and polyamorphism were found in the TiO_2 nanotubes. We discussed the effects of morphology and size on the high pressure phase transition behaviors for the TiO_2 nanotubes.

II. EXPERIMENT

The anatase TiO_2 nanotubes were synthesized by a simple hydrothermal synthesis route as described in our previous work.[22] Briefly, 0.5 g of TiO_2 (Degussa P25) powders and 14 mL of 10 M NaOH aqueous solution were mixed and sealed in a 18 mL autoclave. The mixture was heated to 180 °C for 4 h in the autoclave. After acid washing, the intermediate hydrogen titanate nanotubes were calcined at 400 °C for 4 h, resulting in the formation of anatase TiO_2 nanotubes. The morphology of the nanotubes was characterized by high resolution transmission electron microscopy (HRTEM) (JEM-2200FS). In situ angle-dispersive synchrotron XRD measurements under high pressure were performed at the X17C beamline of Brookhaven National Laboratory. The incident wavelength of the monochromatic X-ray beam was 0.4066 Å. Part of the X-ray diffraction experiments were carried out at 4W2 beamline of Beijing Synchrotron Radiation Facility (BSRF). High pressure was generated by a symmetric diamond anvil cell (DAC) with a pair of diamonds with a culet size of 400 μm. A hole with a diameter of ~150 μm was drilled on a preindented stainless steel gasket and used as the sample chamber. The sample was loaded in the hole with the pressure-transmitting medium of 4:1 methanol-ethanol mixture. The pressures were determined from the pressure-dependent shift of the R1 line fluorescence of ruby. Rietveld refinements of the XRD patterns were conducted using the GSAS software package.[23] The recovered sample in DAC was transferred to a carbon-coated copper grid for TEM and HRTEM observation.

III. RESULTS AND DISCUSSION

Fig. 1 shows the TEM and HRTEM images of the TiO_2 nanotubes. Highly uniform nanotubes with the outer diameters of 8-10 nm and the lengths of several hundred nanometers are observed in Figure 1. From the Fig. 1(b), it can be seen clearly that the nanotubes consist of multiple walls with an inner wall diameters of about 5 nm. Remarkable, the tubes are open ended that are different from the capped carbon nanotubes. There exist a number of defects in the nanotubes that maybe caused by the dehydration process of the heat treatment during the transition from the intermediate hydrogen titanate nanotubes to the anatase TiO_2 nanotubes.[24] As shown in the inset image of Fig. 1(c), the lattice spacing of 0.18 nm corresponds to the (200) planes of anatase TiO_2. This indicates that the nanotube grows along *a* axis. The as-prepared TiO_2 nanotubes agree well with the previous report.[24]

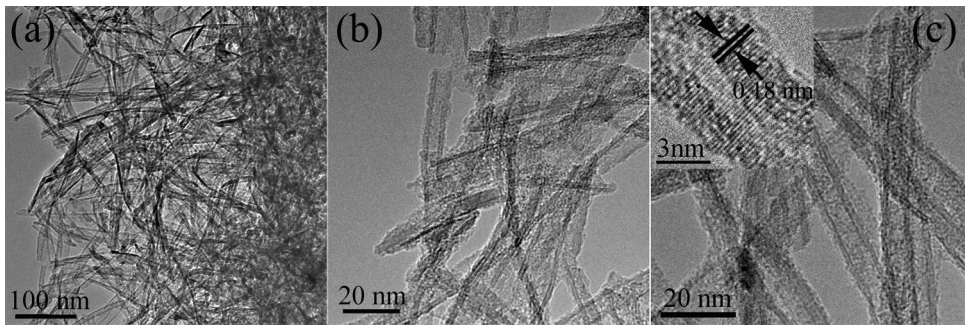

FIG. 1. TEM and HRTEM images of the TiO_2 nanotubes.

At ambient conditions, the anatase TiO_2 nanotubes gave the lattice constants of a = b = 3.795 (1) Å, and c = 9.519 (6) Å, and volume (V) of 137.11 (11) $Å^3$, close to the values observed for bulk material[25] and nanoparticles.[26] The selection of the XRD patterns of the anatase TiO_2 nanotubes is shown in Fig. 2. At low pressure, the diffraction peaks can be indexed to the anatase phase (JCPDS file 21-1272) well, but with obvious broadening because of the ultrafine nanosize of the nanotubes. All the peaks of TiO_2 nanotubes shift to larger angles with increasing pressure, indicating the shrinkage of the unit cells. Upon compression to ~17.9 GPa, a new broad peak characteristic of the baddeleyite phase appears. It indicates that the anatase phase starts to transform into the baddeleyite phase. The phase transition onset pressure is much higher that of bulk counterparts.[25] With further increasing pressure, all peaks of anatase phase disappear and only several broad and weak peaks of baddeleyite phase can be observed above ~25.5 GPa. These weak peaks even further broaden and nearly disappear at the highest pressure of ~35.3 GPa. The phase transition of anatase nanotubes is similar to the pressure-induced amorphization of ultrafine anatase nanocrystals.[19–21] This means that the anatase structure transforms into an amorphous or highly disordered baddeleyite form upon compression. Upon decompression, several broad peaks are observed, which are different from those of the high pressure form (~ 35.3 GPa). These peaks correspond to those of the α-PbO_2 phase. These data suggest that the high pressure form converts into another amorphous or high disordered α-PbO_2 structure upon decompression. It is possible that a transition from a high density amorphous form to a low density amorphous form takes place in the anatase nanotubes under high pressure. The similar ployamorphism also has been observed in ultrafine anatase nanocrystals and TiO_2-B nanoribbons.[13,19]

The lattice parameter ratios (a/a_0 and c/c_0) for the anatase phase nanotubes are shown in Fig. 3 as a function of pressure. The a/a_0 and c/c_0 radios decrease with increasing pressure monotonously. Obviously, the a axis is more compressible than the c axis. This anisotropic compressibility derives from the feature of anatase phase crystal structure, which has been interpreted by the difference in

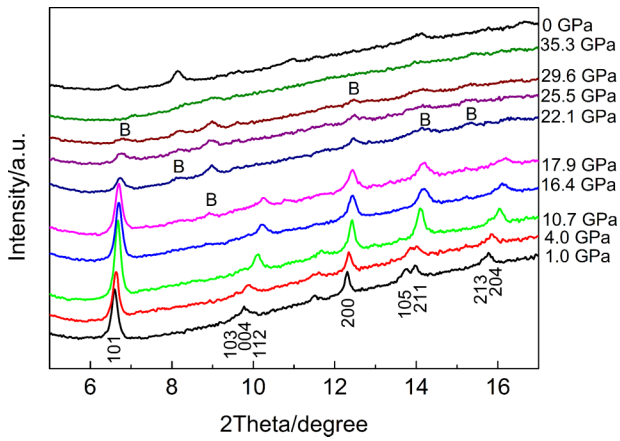

FIG. 2. High pressure XRD patterns of TiO_2 nanotubes at room temperature. The diffraction peaks for baddeleyite phase are marked as B.

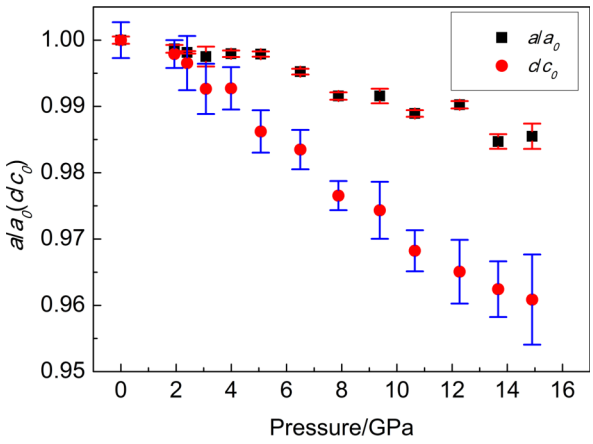

FIG. 3. Pressure dependence of relative lattice parameters (a/a_0, c/c_0) of TiO_2 nanotubes. The squares and circles represent the a/a_0 and c/c_0 for the anatase TiO_2 nanotubes, respectively.

the directional population of the hard occupied TiO_6 and soft empty O_6 octahedra and their relative compressed tendency along a- and c-axes under high pressure.[26]

Fig. 4 shows the pressure-volume data of anataseTiO_2 nanotubes, bulk, nanoparticles, nanorods, nanorices, and nanosheets. The pressure-volume data of the anantase nanotubes was fitted to the third-order Birch-Murnaghan equation of state:

$$P = 3/2B_0[(V/V_0)^{-7/3}\text{-}(V/V_0)^{-5/3}]\{1 + 3/4(B_0'\text{-}4)[(V/V_0)^{-2/3}\text{-}1]\}$$

where V is the volume at pressure P and V_0 is the zero-pressure volume. The constants B_0 and B_0' are the isothermal bulk modulus and its pressure derivative, respectively. As shown in Fig. 4, the fitting to the P-V curve yields a bulk modulus value of B_0 = 166 (9) GPa with the first derivative (B_0') being fixed at 4. The bulk modulus (B_0) of the anatase TiO_2 nanotubes is smaller than those of the corresponding bulks and nanoparticles with different size and morphology (180-319 GPa).[15,25,27,28] We suggest that the reduced bulk modulus of nanotubes can be attributed to their nanotube morphology in which the large shell spacing maybe plays an important role in the high pressure phase transition.

The morphology of the recovered TiO_2 nanotubes was investigated by TEM/HRTEM. As shown in Fig. 5, the quenched samples remain their nanotube morphology intactly. Both the diameter and length show no obvious change, but the shell spacing is undiscernible. It is clear that the spacings of the multiwall nanotubes decrease remarkably during the high pressure phase transitions. From Fig. 5(c), we can see that the long-range ordered crystal structure disappeared and only some short-range ordered domains exist in the nanotubes. The lattice fringes of these domains exhibit a distance of about

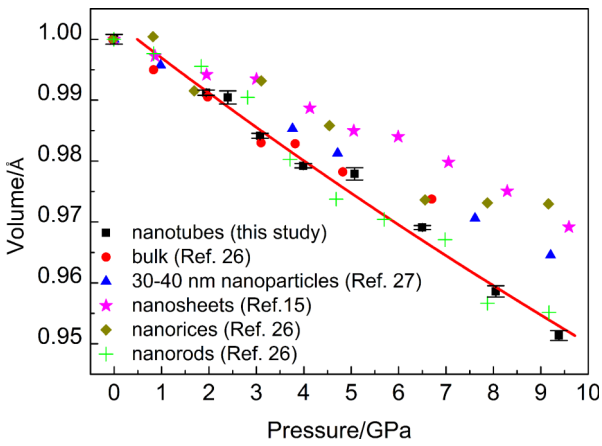

FIG. 4. Pressure-volume diagram of the TiO_2 nanotubes compared with data from bulk (Ref. 26), nanoparticles (Ref. 27), nanorods (Ref. 26), nanorices (Ref. 26), and nanosheets (Ref. 15).

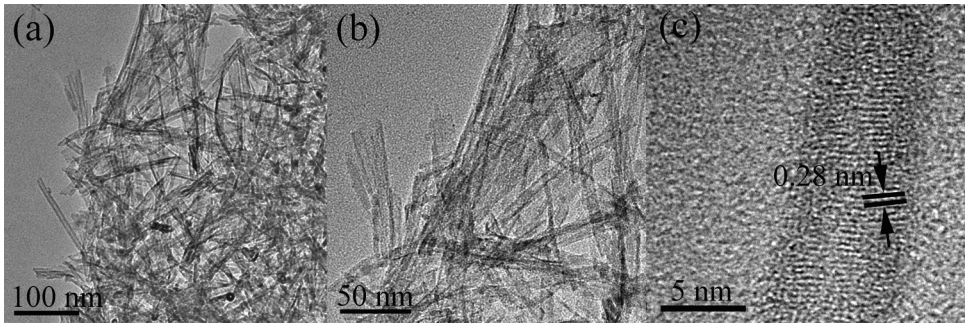

FIG. 5. TEM and HRTEM images of the TiO_2 nanotubes after released from ~35 GPa to ambient pressure.

0.28 nm corresponding to the (111) plane of the α-PbO_2 phase. It is consistent with our XRD results, indicating the LDA TiO_2 nanotubes are obtained at ambient conditions. The HRTEM result demonstrates that the relationship between the LDA form and the α-PbO_2 phase derives from the short-range ordered domains with α-PbO_2 structure. This result further confirms that the HDA-LDA transition occurred in the TiO_2 nanotubes. The similar polyamorphism has been found in ultrafine TiO_2 nanoparticles and one-dimensional TiO_2 nanoribbons.[13,19]

It is well known that the high pressure behaviors of nanomaterials depend on both their size and morphology largely, especially for TiO_2 nanomaterials. Size-induced enhancement of the phase transition pressure was observed in TiO_2 nanocrystals because of their high surface energy.[19,20,27] In addition, size-dependent phase transitions were found in anatase nanocrystals, in which the phase transition mechanism was explained in terms of the higher surface energy for the nanocrystals prohibits the transitions from the starting anatase phase to the high pressure structures.[20] Morphology-tuned anatase-baddeleyite transition was observed in 50-200 nm TiO_2 nanowires, which demonstrates the morphology play an important role in the phase transition.[14] More recently, Dong et al. revealed that both the morphology and dimension of TiO_2 nanowires play a determining role in the high pressure structural transformations.[29] Moreover, Lee et al. found that the shape of TiO_2 nanoparticles show significant modulation effects on the compressibility of the nanoparticles.[26] Ultrahigh bulk modulus (~317 GPa) was obtained in TiO_2 nanosheets with high reactive {001} facets, which can be attributed to the significant nanosize effects in c-axis.[15] In our case, the anatase-baddeleyite transition pressure is much higher than those of nanowires,[14] nanosheets[15] and corresponding bulk,[25] but is close to the PIA pressures of ultrafine nanoparticles.[19–21] Obviously, the large specific surface area and ultrafine nanosize of the nanotubes result in a significant high surface energy, which contributes to the enhanced phase transition pressure. However, the ultrafine size of nanotubes precludes the further phase transition from anatase to baddeleyite. Thus, an amorphous form (HDA) with a structural relation to the baddeleyite was found in the nanotubes under high pressure. Upon decompression, the structural relationship-drived HDA-LDA transition occurred and the LDA TiO_2 nanotubes with a structural relation to the α-PbO_2 phase were obtained. For the reduced bulk modulus of TiO_2 nanotubes, the unique open nanotube morphology and the plenty of crystal defects may be the main reasons which lead to high compressibility for crystal unit cells.

It is very interesting that the nanotube morphology can be preserved under high pressure. It is known that the pore size (inner diameter) of the nanotubes is about 5 nm. Evidently, the pore size is large enough to be penetrated by the transmitting medium of 4:1 methanol-ethanol mixture. In our experiment, the transmitting medium penetrates into the channels of the nanotubes forming a homogenous condition between inner and outer walls. Under high pressure, the inner transmitting medium plays a supporting role and prevents the collapse of the nanotubes. Our previous works have shown that the TiO_2 nanoribbons,[13] nanowires,[14] nanoporous structures[15] and nanosheets[16] with high pressure phase or amorphous form can be prepared by the high pressure treatment. Here, our results further demonstrate that new amorphous TiO_2 nanotubes can be obtained by the high pressure method. It also confirms that high pressure is an effective way to prepare complicated nanomaterials with new structures.

IV. CONCLUSION

In summary, LDA TiO_2 nanotubes with diameters of 8-10 nm and length of several nanometers were synthesized successfully by high pressure treatment of anatase TiO_2 nanotubes. The structural phase transitions and morphology change of anatase TiO_2 nanotubes were studied by in-situ high-pressure synchrotron XRD and TEM (HRTEM) techniques. A phase transition from the initial anatase structure to an HDA form related to baddeleyite phase occurred at above 25.5 GPa. The PIA-induced HDA form converts into an LDA-TiO_2 polyamorph during decompression. The LDA TiO_2 nanotubes were retained at ambient conditions. HRTEM results revealed that the LDA phase is a long-range disordered and short-range ordered α-PbO_2 structure. A bulk modulus B_0 = 158 (9) GPa for the anatase nanotubes is derived from the PV data, which is smaller than those of the corresponding nanoparticles and bulk. These unique high pressure behaviors of TiO_2 nanotubes can be attributed to their open-ended nanotube morphology and ultrafine nanosize.

ACKNOWLEDGMENTS

This work was supported financially by the National Basic Research Program of China (2011CB808200), the NSFC (11374120, 11004075, 10979001, 51025206, 51032001, and 21073071), and the Cheung Kong Scholars Programme of China. This research was partially supported by COMPRES, the Consortium for Materials Properties Research in Earth Sciences under NSF Cooperative Agreement EAR 06-49658.

[1] R. H. Baughman, C. X. Cui, A. A. Zakhidov, Z. Lqbal, J. N. Barisi, G. M. Spinks, G. G. Wallace, A. Mazzoldi, D. D. Rossi, A. G. Rinzler, O. Jaschinski, S. Roth, and M. Kertesz, Science **284**, 1340-1344 (1999).
[2] D. Tasis, N. Tagmatarchis, A. Bianco, and M. Prato, Chem. Rev. **106**, 1105-1136 (2006).
[3] P. Roy, S. Berger, and P. Schmuki, Angew. Chem. Int. Ed. **50**, 2909-2939 (2011).
[4] H. Zhang, G. R. Li, L. P. An, T. Y. Yan, X. P. Gao, and H. Y. Zhu, J. Phys. Chem. C **111**, 6143-6148 (2007).
[5] J. Qu, J. E. Cloud, Y. A. Yang, J. N. Ding, and N. Y. Yuan, ACS Appl. Mater. Interfaces **6**, 22199-22208 (2014).
[6] C. A. Grimes, J. Mater. Chem. **17**, 1451-1457 (2007).
[7] G. K. Mor, K. Shankar, M. Paulose, O. K. Varghese, and C. A. Grimes, Nano Lett. **6**, 215-218 (2006).
[8] S. D. Perera, R. G. Mariano, K. Vu, N. Nour, O. Seitz, Y. Chabal, and K. J. Balkus, ACS Catal. **2**, 949-956 (2012).
[9] H. H. Huo, Z. D. Xu, T. Zhang, and C. L. Xu, J. Mater. Chem. A **11**, 5882-5888 (2015).
[10] X. Xu, Z. Y. Fan, S. J. Ding, D. M. Yu, and Y. P. Du, Nanoscale **10**, 5245-5250 (2014).
[11] Y. J. Tian, B. Xu, D. L. Yu, Y. M. Ma, Y. B. Wang, Y. B. Jiang, W. T. Hu, C. C. Tang, Y. G. Gao, K. Luo, Z. S. Zhao, L. M. Wang, B. Wen, J. L. He, and Z. Y. Liu, Nature **493**, 385-388 (2013).
[12] Q. Huang, D. L. Yu, B. Xu, W. T. Hu, Y. M. Ma, Y. B. Wang, Z. S. Zhao, B. Wen, J. L. He, Z. Y. Liu, and Y. J. Tian, Nature **510**, 250-253 (2014).
[13] Q. J. Li, B. B. Liu, L. Wang, D. M. Li, R. Liu, B. Zou, T. Cui, G. T. Zou, Y. Meng, H. K. Mao, Z. X. Liu, J. Liu, and J. X. Li, J. Phys. Chem. Lett. **1**, 309 (2010).
[14] Q. J. Li, B. Y. Cheng, X. Yang, R. Liu, B. Liu, J. Liu, Z. Q. Chen, B. Zou, T. Cui, and B. B. Liu, J. Phys. Chem. C **117**, 8516-8521 (2013).
[15] Q. J. Li, B. Y. Cheng, B. L. Tian, R. Liu, B. Liu, F. Wang, Z. Q. Chen, B. Zou, T. Cui, and B. B. Liu, RSC Adv. **4**, 12873-12877 (2014).
[16] X. Yang, Q. J. Li, Z. D. Liu, X. Bai, H. W. Song, M. G. Yao, B. Liu, R. Liu, C. Gong, S. C. Lu, Z. Yao, D. M. Li, J. Liu, Z. Q. Chen, B. Zou, T. Cui, and B. B. Liu, J. Phys. Chem. C **117**, 8503-8508 (2013).
[17] Z. W. Quan, Z. P. Luo, Y. X. Wang, H. W. Xu, C. Y. Wang, Z. W. Wang, and J. Y. Fang, Nano Lett. **8**, 3729-3735 (2013).
[18] L. Wang, W. G. Yang, Y. Ding, Y. Ren, S. G. Xiao, B. B. Liu, S. V. Sinogeikin, Y. Meng, D. J. Gosztola, G. Y. Shen, R. J. Hemley, W. L. Mao, and K. K. Mao, Phys. Rev. Lett. **105**, 095701 (2010).
[19] V. Swamy, A. Kuznetsov, L. S. Dubrovinsky, P. F. McMillan, V. B. Prakapenka, G. Y. Shen, and B. C. Muddle, Phys. Rev. Lett. **96**, 135702 (2006).
[20] G. R. Hearne, J. Zhao, A. M. Dawe, V. Pischedda, M. Maaza, M. K. Nieuwoudt, P. Kibasomba, O. Nemraoui, J. D. Comins, and M. J. Witcomb, Phys. Rev. B **70**, 134102 (2004).
[21] V. Swamy, A. Y. Kuznetsov, L. S. Dubrovinsky, A. Kuznetsov, and V. B. Prakapenka, Phys. Rev. Lett. **103**, 075505 (2009).
[22] Q. J. Li, R. Liu, B. Zou, T. Cui, and B. B. Liu, Physica B. **445**, 42-47 (2014).
[23] B. H. Toby, J. Appl. Crystallogr. **34**, 210-213 (2001).
[24] A. Rendon-Rivera, J. A. Toledo-Antonio, M. A. Cortes-Jacome, and C. Angeles-Chavez, Catal. Today **166**, 18-24 (2011).
[25] T. Arlt, M. Bermejo, M. A. Blanco, L. Gerward, J. Z. Jiang, J. Staun Olsen, and J. M. Recio, Phys. Rev. B **6**, 14414 (2000).
[26] S. W. Park, J. T. Jang, J. Cheon, H. H. Lee, D. R. Lee, and Y. Lee, J. Phys. Chem. C **112**, 9627-9631 (2008).
[27] V. Swamy, L. S. Dubrovinsky, N. A. Dubrovinskaia, A. S. Simionovici, M. Drakopoulos, V. Dmitriev, and H. Weber, Solid State Comm. **125**, 111-115 (2003).
[28] V. Pischedda, G. R. Hearne, A. M. Dawe, and J. E. Lowther, Phys. Rev. Lett. **96**, 035509 (2006).
[29] Z. H. Dong and Y. Song, Can. J. Chem. **93**, 165-172 (2015).